Low pressure occurrence during hydrodynamic impact of an elliptic paraboloid entering with arbitrary kinematics.

Y.-M. Scolan
ENSTA-Bretagne
LBMS/DFMS
Brest, FRANCE
yves-marie.scolan@ensta-bretagne.fr

A. A. Korobkin
University of East Anglia
School of Mathematics
Norwich, UK
a.korobkin@uea.ac.uk

***Abstract*—The hydrodynamic impact problem is posed in the frame of the linearized Wagner theory. The so-called flat disk approximation is used. The penetrating body is an elliptic paraboloid. The pure vertical entry is well known and exact solutions exist. When, after hitting the fluid, the body moves along its 5 other degrees of freedom, exact solutions are still available provided the angular motions are small enough. In case of a pure translational motions (both vertical and horizontal) it is possible to determine occurence of low pressure on the wetted surface either in free drop tests or constant velocity penetration.**

I. Introduction

The linearized three-dimensional Wagner problem is known as a mixed Boundary Value Problem posed in Potential Theory. The linearization follows from the asumption that the relative body shape and free surface shape are flat enough. That is measured by the deadrise angle which cannot be smaller than 4^o and greater than 20^o. Mathematically the Boundary Value Problem is posed in a half space, say $z < 0$, and the plane $z = 0$ is described by the cartesian coordinates (x, y), and it contains the free surface $\mathrm{FS}(t)$ and the expanding wetted surface $\mathrm{D}(t)$, as illustrated in (Fig. 1)

II. Theoretical developments

The flow is described with a velocity potential φ which verifies the Laplace equation. The impermability condition on the wetted surface leads to a Neumann condition; the normal velocities of both the fluid and the body are continuous. On the free surface, by neglecting gravity and surface tension effects, the linearized Bernoulli equation reduces to a homogeneous Dirichlet condition. The Boundary Value Problem hence reads

$$\begin{cases} \Delta\varphi = 0 & z < 0 \\ \varphi = 0 & z = 0,\ (x,y) \in \mathrm{FS}(t) \\ \varphi_{,z} = -W(t) & z = 0,\ (x,y) \in \mathrm{D}(t) \\ \varphi \to 0 & (x^2+y^2+z^2) \to \infty, \end{cases} \tag{1}$$

The regularity of the solution is increased by using the displacement potential ϕ which is the time integral of the velocity potential φ. The Boundary Value Problem written for the displacement potential remains unchanged except the Neumann condition on $\mathrm{D}(t)$, which now reads

$$\phi_{,z} = -h(t) + f(x,y), \quad h(t) = \int_0^t W(\tau)d\tau \tag{2}$$

where the right hand side is the distance between a point on the body and the undisturbed free surface, that is to say its vertical displacement. Let us consider an elliptic paraboloid described in a Cartesian local coordinate system (O, X, Y, Z) as illustrated in (Fig. 2). Its equation is

$$Z = f(X,Y) = \frac{X^2}{2r_x} + \frac{Y^2}{2r_y} \tag{3}$$

where (r_x, r_y) are the curvature radii. Alternatively we can use the coefficients $A^2 = 2r_x$ and $B^2 = 2r_y$. We consider that the body penetrates the free surface not only with a vertical velocity but also with horizontal velocities along its two axis $X = 0$ and $Y = 0$ as described in (Fig. 3) We denote (U, V, W) the Cartesian components of the body velocity. The motion is described in a coordinate system attached to earth

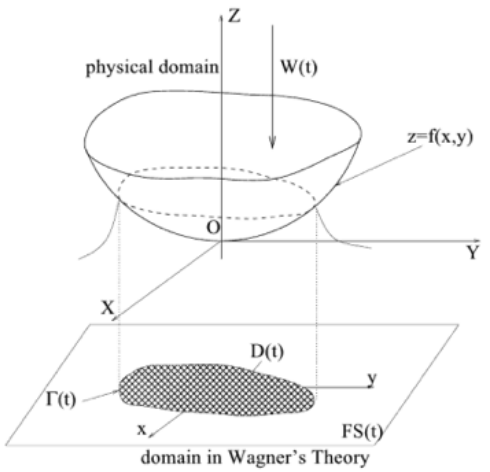

Fig. 1. Illustration of the linearized three-dimensional Wagner problem.

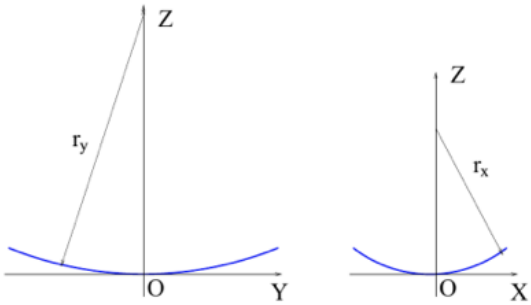

Fig. 2. Cut of the elliptic paraboloid by the vertical planes $X = 0$ (left) and $X = 0$ (right).

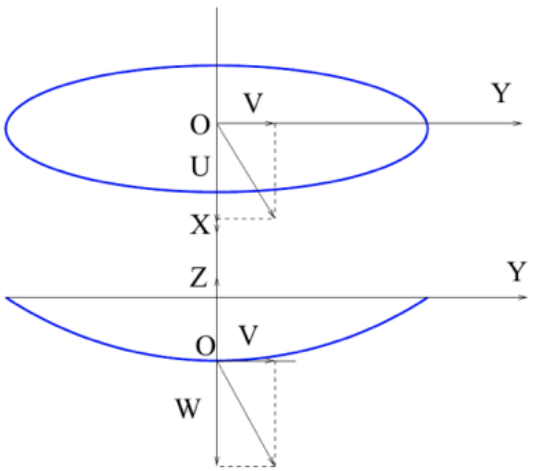

Fig. 3. Kinematics of the elliptic paraboloid with vertical and horizontal velocity components.

(A, x, y, z) which coincides with the Cartesian coordinate system (O, X, Y, Z) at initial time $t = 0$. In the system attached to earth, the coordinates of a point on the wetted surface, are thus

$$x = X + \int_0^t U(\tau)d\tau = X + \delta x(t) \tag{4}$$

$$y = Y + \int_0^t V(\tau)d\tau = Y + \delta y(t), \tag{5}$$

$$z = Z - \int_0^t W(\tau)d\tau = Z - h(t) \tag{6}$$

At any instant the vertical displacement of a point on the wetted surface is hence

$$\phi_{,z} = -h(t) + \frac{(x - \delta x(t))^2}{2r_x} + \frac{(y - \delta y(t))^2}{2r_y} \tag{7}$$

That means that the right hand side of the Neumann condition remains unchanged provided that we use the change of variables

$$\tilde{x} = x - \delta x(t), \quad \tilde{y} = y - \delta y(t), \quad \tilde{z} = z \tag{8}$$

The Boundary Value Problem is re-written for $\tilde{\phi}(\tilde{x}, \tilde{y}, \tilde{z}, t) = \phi(x, y, z, t)$ as follows

$$\begin{cases} \Delta\tilde{\phi} = 0 & \tilde{z} < 0 \\ \tilde{\phi} = 0 & \tilde{z} = 0,\ (\tilde{x}, \tilde{y}) \in \mathrm{FS}(t) \\ \tilde{\phi}_{,\tilde{z}} = -h(t) + f(\tilde{x}, \tilde{y}) & \tilde{z} = 0,\ (\tilde{x}, \tilde{y}) \in \mathrm{D}(t) \\ \tilde{\phi} \to 0 & (\tilde{x}^2 + \tilde{y}^2 + \tilde{z}^2) \to \infty, \end{cases} \tag{9}$$

and a standard boundary value problem is obtained. As proved in [3], the displacement potential is also the solution of the integral equation

$$\frac{1}{2\pi} \int_{D(t)} \frac{\Delta_2\tilde{\phi}\ \mathrm{d}s_0}{||M\vec{M}_0||} = h(t) - f(\tilde{x}, \tilde{y}), \tag{10}$$

with the additional boundary conditions

$$\tilde{\phi} = 0, \quad \text{and} \quad \tilde{\phi}_{,n} = 0, \quad \text{at } \Gamma(t) = D(t) \cap FS(t). \tag{11}$$

The integrand of (10) is studied by [8]. In particular it is proved that $\Delta_2\tilde{\phi}$ is singular as the inverse square root of the distance to $\Gamma(t)$. In other words $\Delta_2\tilde{\phi}$ can be written

$$\Delta_2\tilde{\phi} = \frac{s(\tilde{x}, \tilde{y}, t)}{\sqrt{F(\tilde{x}, \tilde{y}, t)}} \tag{12}$$

where s is regular on $\mathrm{D}(t)$ and the function F vanishes along the contact line $\Gamma(t)$. It is conjectural whether or not F is the equation of an ellipse in the plane $(\tilde{x}, \tilde{y})$ knowing that the shape is an elliptic paraboloid. Indeed, that result is proved in [6]: an elliptic paraboloid entering fluid with arbitrary vertical velocity yields an elliptic wetted surface as well. The function F can hence be expressed as

$$F(\tilde{x}, \tilde{y}, t) = 1 - \frac{\tilde{x}^2}{a^2} - \frac{\tilde{y}^2}{b^2} \tag{13}$$

Then we can invoke Galin's theorem (see appendix A) The application of this theorem to the present case is detailed in [7]. In particular a closed form expression of the displacement potential is obtained

$$\phi(\tilde{x}, \tilde{y}, t) = -\frac{2ha}{3E}\left(1 - \frac{\tilde{x}^2}{a^2} - \frac{\tilde{y}^2}{b^2}\right)^{3/2} \tag{14}$$

That result proves that the displacement potential varies linearly with the penetration depth. No special assumptions are made regarding the kinematics of the entering body. The expression of the velocity potential follows from

$$\varphi = \frac{d\phi}{dt} = -\frac{aU}{E}\sqrt{1 - \frac{\tilde{x}^2}{a^2} - \frac{\tilde{y}^2}{b^2}} \tag{15}$$

which is consistent with the result of [4]. Galin's theorem allows to prove that the aspect ratio of the elliptic wetted surface (noted k) is uniquely defined by the aspect ratio of the elliptic paraboloid (noted k_γ), according to

$$k_\gamma^2 = \frac{A^2}{B^2} = \frac{r_x}{r_y} = k^2\frac{1 + k^2 D/E}{2 - k^2 D/E} \tag{16}$$

whose variation is plotted in figure (Fig. 4).

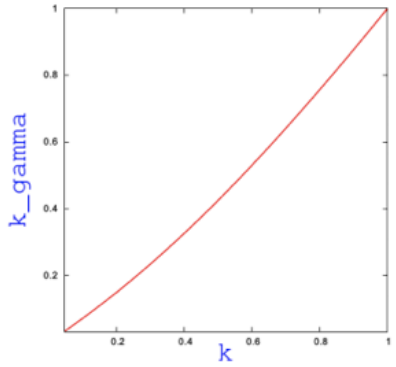

Fig. 4. Variation of k_γ with k; see equation (16).

Here E and K are Elliptic Functions of the eccentricity $e=\sqrt{1-k^2}$

$$E(e)=\int_0^{\pi/2}\sqrt{1-e^2\sin^2\theta}d\theta \tag{17}$$

$$K(e)=\int_0^{\pi/2}\frac{d\theta}{\sqrt{1-e^2\sin^2\theta}},\quad D=(K-E)/e^2 \tag{18}$$

$$b=B\sqrt{h\left(1+k^2\frac{D}{E}\right)}=\eta\sqrt{h} \tag{19}$$

$$a=A\sqrt{h\left(2-k^2\frac{D}{E}\right)} \tag{20}$$

It is worth noting that the lengths of the semi-axes, at any instant of penetration, are proportional to the square root of the penetration depth h. Finally we can retrieve the expression of the displacement potential in the coordinate system attached to earth

$$\phi(x,y,t)=-\frac{2ha}{3E}\left(1-\frac{(x-\delta x)^2}{a^2}-\frac{(y-\delta y)^2}{b^2}\right)^{3/2} \tag{21}$$

That result is essential in order to properly determine the pressure.

III. Hydrodynamic loads

A. Pressure formulation

The pressure follows from the linearized Bernoulli equation

$$p=-\rho\varphi_{,t}=-\rho\phi_{,t^2} \tag{22}$$

The time derivatives in (22) make the expression of the pressure rather complicated. In order to illustrate its variation in space and time, we consider an elliptic paraboloid which enters the free surface with vertical velocity $W=\dot{h}$ and the horizontal components $U=\dot{\delta x}$ and $V=\dot{\delta y}$. Here are some details of the time derivatives

$$\phi_{,t}=-\frac{\sqrt{F}}{E}\left(\frac{2}{3}\frac{\dot{}}{ha}F+ha\dot{F}\right) \tag{23}$$

$$F=1-\frac{(x-\delta x)^2}{a^2}-\frac{(y-\delta y)^2}{b^2} \tag{24}$$

$$\dot{F}=\frac{2(x-\delta x)U}{a^2}+\frac{2(y-\delta y)V}{b^2}+ +\frac{2\dot{a}(x-\delta x)^2}{a^3}+\frac{2\dot{b}(y-\delta y)^2}{b^3} \tag{25}$$

By using the identities

$$2h\dot{a}=\dot{h}a,\quad \frac{\dot{a}}{a}=\frac{\dot{b}}{b} \tag{26}$$

it remains

$$\phi_{,t}=-\frac{M\sqrt{F}}{E} \tag{27}$$

$$M=Wa+2ah\frac{(x-\delta x)U}{a^2}+2ah\frac{(y-\delta y)V}{b^2} \tag{28}$$

To go further we need $\dot{M}$, yielding

$$\dot{M}=\dot{\overline{aW}}-2ah\left(\frac{U^2}{a^2}+\frac{V^2}{b^2}\right)+ +\frac{2(x-\delta x)}{a^2}\left(ah(\dot{U}-\frac{2\dot{a}}{a}U)+\dot{\overline{ah}}U\right)+ +\frac{2(y-\delta y)}{b^2}\left(ah(\dot{V}-\frac{2\dot{b}}{b}V)+\dot{\overline{ah}}V\right) \tag{29}$$

and finally the pressure reads

$$p=\frac{\rho}{E\sqrt{F}}\left(\dot{M}F+\frac{1}{2}M\dot{F}\right) \tag{30}$$

We can already anticipate that the pressure distribution over the wetted surface will be substantially different than for the pure vertical entry.

B. Spatial and temporal variations of the pressure

We focus on the variation of the pressure in space and time. More precisely we can determine the location of possible change of sign of the pressure. As an illustration, the quantity $P=\frac{pE\sqrt{F}}{\rho}$ is expressed along the axis of the y-translational motion. We reduce the motion of the entering body to sway $U=0$. The coordinate $Y=\frac{y-\delta y(t)}{b}$ is such that $|Y|<1$ on the wetted surface. The pressure is expressed as follows

$$P(Y)=Q(t,Y)(1-Y^2)+\frac{Y}{b}(V+\dot{b}Y)\left(Wa+2hkYV\right) \tag{31}$$

with

$$Q(t,Y)=\dot{\overline{Wa}}-\frac{2ahV^2}{b^2}+\frac{2Y}{b}\left(V\dot{\overline{ah}}+ah(\dot{V}-\frac{2\dot{b}}{b}V)\right) \tag{32}$$

It is noticeable that at the contact point $Y=-1$ (*i.e.* at the stern), the pressure vanishes if the velocity of expansion of the wetted surface $\dot{b}$ is set to the translational velocity V. That happens at a given instant. By using the expression (26) and assuming that V and W are constant, this instant is

$$t_{P(-1)=0}=\frac{\eta^2W}{4V^2}=\frac{B^2W}{4V^2}\left(1+k^2\frac{D}{E}\right) \tag{33}$$

with the notation of equation (19). The pressure can remain negative over a significant region of the wetted surface. As an example, we consider the elliptic paraboloid entering with constant velocities (V, W). We introduce $m = \frac{2Vh}{bW} = \frac{V}{b}$ which appears as a nondimensional measure of time $m = \frac{2V}{\eta}\sqrt{\frac{t}{W}}$. The pressure (31) reduces to

$$P(Y) = kVW\left(2mY^2 + 2Y + \frac{1}{m} - m\right) \qquad (34)$$

(Fig. 5) shows the variation of $\frac{P}{kVW}$ with m and Y The

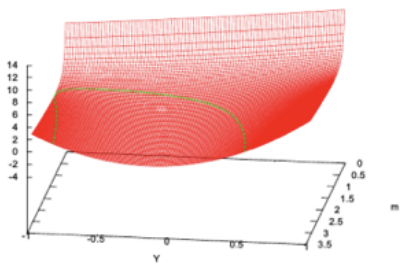

Fig. 5. Variation of $\frac{P}{kVW}$ with m and Y according to equation (34) when velocities (V, W) are constant in time.

superposed line separates the plane (Y, m) in two areas, one of them corresponds to negative pressure. Above a critical coefficient $m_{crit.} = 1/\sqrt{2}$, $P(Y)$ has zeroes and becomes negative. Figure (6) shows (in logscale) the variation of $\frac{P}{kVW}$ (from equation 34) as $m < m_{crit.}$.

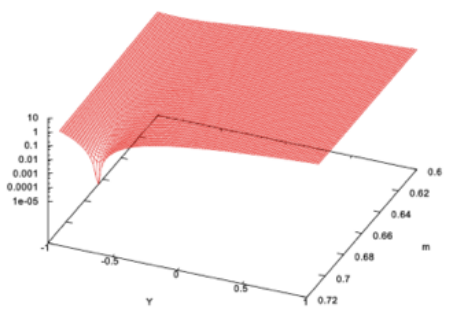

Fig. 6. Logscale variation of $\frac{P}{kVW}$ with $m < m_{crit.}$ and Y according to equation (34) when velocities (V, W) are constant in time.

It is shown that the first zero appears at $Y = -1/\sqrt{2}$. Note that the Wagner model of water impact can be used only during the initial stage when the pressure is either positive everywhere in the contact region or negative strictly inside this region. After the time instant (given by equation 33)), when the zone of negative pressures approaches the contact line, Wagner's model cannot be used and another model should be employed.

C. *Analysis of the pressure peak*

The pressure in (30) is said of first order. Its singularity behaves like the inverse square root of the distance to the contact line, where $F = 0$. The matching of this solution to a local solution at the spray root is commonly used to propose a uniformly bounded distribution of pressure. Then it is possible to capture its maximum. The twodimensional jet root solution is described by [13]. The asymptotics of the velocity potential (ϕ_{root}) and the pressure (P_{root}) along the contact line Γ require the introduction of velocity V_j of fluid in the jet and the thickness of the jet d

$$\phi_{root} = -4V_j\sqrt{\frac{d\xi}{\pi}}, \qquad P_{root} = 2\rho V_j^2\sqrt{\frac{d}{\pi\xi}} \qquad (35)$$

where ξ is the distance between a point $(a\cos\alpha, b\sin\alpha)$ at the contact line and a point (X_Q, Y_Q) on the wetted surface along the normal $\vec{N}$ to the contact line

$$\vec{N} = -\frac{\vec{\nabla}F}{||\vec{\nabla}F||} = \frac{1}{\sqrt{\cos^2\alpha + k^2\sin^2\alpha}}\begin{pmatrix}\cos\alpha\\ k\sin\alpha\end{pmatrix} \qquad (36)$$

Figure (Fig. 7) illustrates those notations. As a first step, we

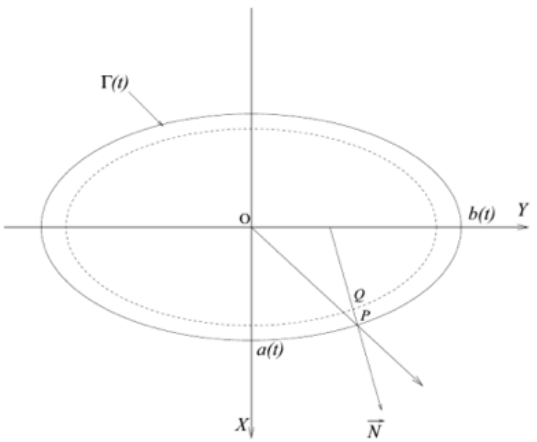

Fig. 7. Notations for the description of the flow at the contact line.

use a Taylor development to express F in (23), $\dot{F}$ in (25) and M in (27) asymptotically at point Q close to the contact line, *i.e.* as ξ is small.

$$M_{asymp} = Wa + 2h(U\cos\alpha + kV\sin\alpha) + O(\xi) \qquad (37)$$

$$F_{asymp} = \frac{2\xi}{a}\sqrt{\cos^2\alpha + k^2\sin^2\alpha} + O(\xi^2) \qquad (38)$$

$$\dot{F}_{asymp} = \frac{W}{h} + \frac{2}{a}(U\cos\alpha + kV\sin\alpha) + O(\xi) \qquad (39)$$

Introducing these last expressions in (30) and (23) and matching the resulting velocity potential and pressure with (35) yields the fluid velocity in the jet V_j and the thickness of the jet d as follows

$$V_j = \frac{1}{2h}\frac{Wa + 2h(U\cos\alpha + kV\sin\alpha)}{\sqrt{\cos^2\alpha + k^2\sin^2\alpha}} \qquad (40)$$

$$d = \frac{\pi h^2}{2aE^2}(\cos^2\alpha + k^2\sin^2\alpha)^{3/2} \quad (41)$$

It is shown that the jet thickness does not depend on the horizontal motion. This matching also provides the measure of the pressure peak

$$p_{max} = \frac{\rho}{8h^2}\frac{(Wa + 2h(U\cos\alpha + kV\sin\alpha))^2}{\cos^2\alpha + k^2\sin^2\alpha} \quad (42)$$

As a example, we determine this peak for translational motion along the Y axis ($U = 0$), yielding

$$p_{U=0} = \frac{1}{2}\rho V^2\left(1 + \frac{\sin\alpha}{m}\right) \quad (43)$$

It is shown that the maximum is higher at the stern than at the bow part of the elliptic paraboloid.

D. MLM for the pressure

MLM stands for Modified Logvinovich Model. It has been introduced by [9] in order to improve the prediction of the hydrodynamic force. However the equations can be rapidly heavy if we treat the general 6dof motion. That is why we keep horizontal translational motion only.

As a starting point we express the impermeability condition on the body surface in terms of the velocity potential φ which is the 3D solution describing the flow about the actual shape

$$\vec{\nabla}\varphi \cdot \vec{n} = \vec{v} \cdot \vec{n} \quad (44)$$

where $\vec{n}$ is the exact normal unit vector on the wetted surface and $\vec{v}$ is the velocity of the body

$$\vec{v} = -W\vec{z} + U\vec{x} + V\vec{y} \quad (45)$$

Knowing the instantaneous body position,

$$z = f(x - \delta x, y - \delta y) - h(t) = f^\star(x, y, t) - h(t) \quad (46)$$

we hence determine the normal velocity on the body surface

$$\vec{\nabla}\varphi \cdot \vec{n} = \frac{1}{\sqrt{1 + \vec{\nabla}^2 f}}\left(\varphi_{,x}f_{,x} + \varphi_{,y}f_{,y} - \varphi_{,z}\right)$$

$$= \frac{1}{\sqrt{1 + \vec{\nabla}^2 f}}\left(\vec{\nabla}_{(x,y)}\varphi \cdot \vec{\nabla} f - \varphi_{,z}\right) \quad (47)$$

and the vertical velocity follows

$$\varphi_{,z} = \vec{\nabla}\varphi \cdot \vec{\nabla} f - \vec{v} \cdot \vec{\nabla} f - W \quad (48)$$

We introduce the velocity potential Φ

$$\Phi(x, y, t) = \varphi(x, y, f^\star(x, y, t) - h(t), t) \quad (49)$$

from which we calculate the time derivative

$$\Phi_{,t} = \varphi_{,t} - \varphi_{,z}\left(\vec{v} \cdot \vec{\nabla} f + W\right) \quad (50)$$

and its spatial derivatives

$$\vec{\nabla}\Phi = \vec{\nabla}_{(x,y)}\varphi + \varphi_{,z}\vec{\nabla} f \quad (51)$$

yielding

$$\varphi_{,z} = \frac{1}{D}\left(\vec{\nabla}\Phi \cdot \vec{\nabla} f - \vec{v} \cdot \vec{\nabla} f - W\right), \quad D = 1 + \vec{\nabla}^2 f \quad (52)$$

We get the final expression of the reduced pressure $P(x, y, t) = p(x, y, f^\star(x, y, t) - h(t), t)$

$$-\frac{1}{\rho}P(x, y, t) = \Phi_{,t} + \frac{1}{2}\vec{\nabla}^2\Phi - \frac{1}{2}(1 + \vec{\nabla}^2 f)\varphi_{,z}^2 \quad (53)$$

It remains to calculate the solution Φ from the Taylor development

$$\varphi(x, y, z, t) = \varphi(x, y, 0, t) + z\varphi_{,z}(x, y, 0, t) + ...$$
$$\text{at} \quad z = f^\star(x, y, t) - h(t) \quad (54)$$

where $\varphi(x, y, 0, t)$ is the solution of the linearized Wagner model noted $\varphi^{(l)}$ and its vertical derivative on the body surface is $\varphi_{,z}(x, y, 0, t) \approx \varphi_{,z}^{(l)}(x, y, 0, t) = -W$

$$\Phi(x, y, t) = \varphi^{(l)} - W\Big[f^\star(x, y, t) - h(t)\Big] \quad (55)$$

where $\varphi^{(l)}$ is given by equation (27). Its time and spatial derivative are then expressed as

$$\varphi_{,t}^{(l)} = -\frac{1}{E}\left(\sqrt{F}\dot{M} + \frac{M\dot{F}}{2\sqrt{F}}\right) \quad (56)$$

$$\vec{\nabla}\varphi^{(l)} = -\frac{1}{E}\left(\sqrt{F}\vec{\nabla}M + \frac{M\vec{\nabla}F}{2\sqrt{F}}\right) \quad (57)$$

which are used in

$$\Phi_{,t} = \varphi_{,t}^{(l)} - \dot{W}(f^\star - h) + W(\vec{v} \cdot \vec{\nabla} f + W) \quad (58)$$

$$\vec{\nabla}\Phi = \vec{\nabla}\varphi^{(l)} - W\vec{\nabla} f \quad (59)$$

Finally the MLM pressure with horizontal velocity reads

$$-\frac{1}{\rho}P(x, y, t) = \varphi_{,t}^{(l)} - \dot{W}(f^\star - h) + \frac{1}{2}W^2 + \frac{1}{2}\vec{\nabla}^2\varphi^{(l)}$$
$$-\frac{1}{2D}\left((\vec{\nabla}\varphi^{(l)} - \vec{v}) \cdot \vec{\nabla} f\right)^2 \quad (60)$$

In order to compare the pressure (60) to the first order pressure (30), we consider a practical case of an elliptic paraboloid with curvature radii $r_x = \sqrt{A} = 0.75m$ and $r_y = \sqrt{B} = 2m$ respectively in the two horizontal directions x and y. It enters vertically with velocity $W = 1m/s$ and the horizontal velocity along the y axis varies from $V = 0m/s$ up to $V = 10m/s$. The pressure is measured with the sensor of finite size. Its area is circular with radius $r_s = 0.0025m$. Figures (Fig. 8) and (Fig. 9) show the influence of the horizontal velocity on the pressure at two points along the axis of motion, $|Y| = 0.05m$ (Fig. 8) and $|Y| = 0.20m$ (Fig. 9). The effect of the pressure averaging over the sensor area is clear. Without this averaging, we would get rather unphysical sharp peaks. It is shown that the pressure is higher on the upstream side than along the downstream side. The case with a zero horizontal velocity $V = 0m/s$ is intermediate between the pressures measured at both sides. It is worth reminding that the pressure maximum

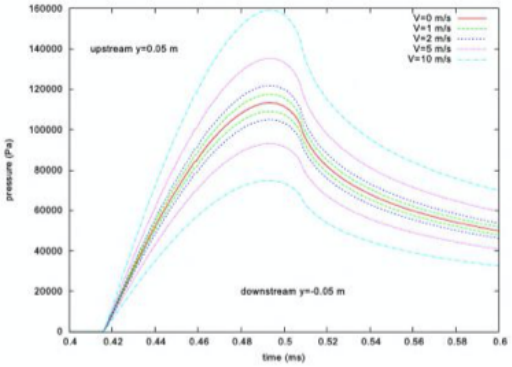

Fig. 8. Time variation of the pressure measured by a pressure sensor located at $|Y| = 0.05m$ along the major semi-axis. The sensor is circular with radius $r_\theta = 0.0025m$.

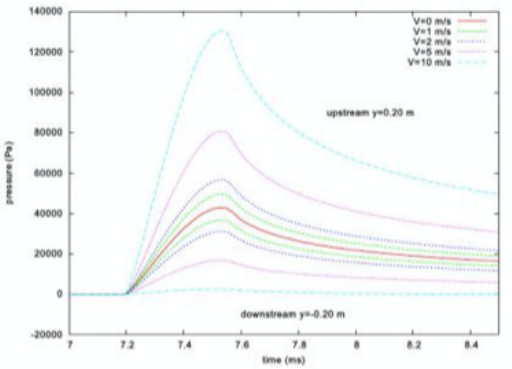

Fig. 9. See caption in (Fig. 9); the pressure sensor located at $|Y| = 0.20m$.

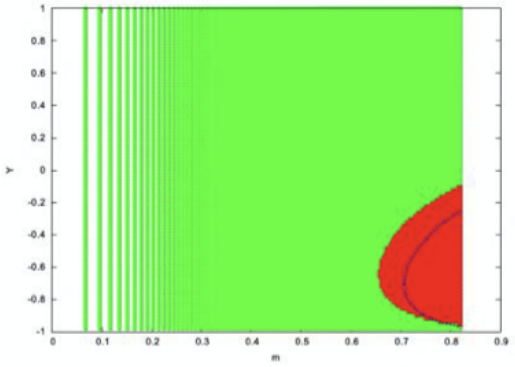

Fig. 10. Variation of the MLM pressure in terms of m and Y for a horizontal velocity $V = 5m/s$. The superimposed line: zero of the first order pressure (34).

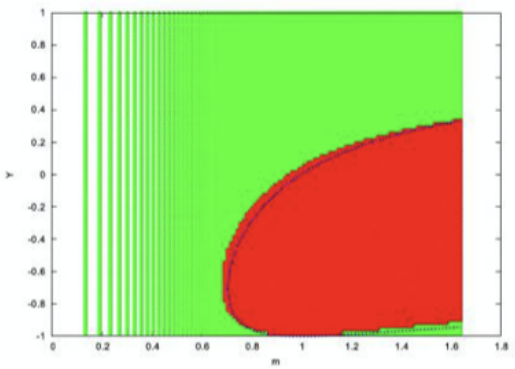

Fig. 11. See caption in (Fig. 10). Horizontal velocity $V = 10m/s$.

is evaluated without reference to the inner solution as in (42). The fact that dynamics of expansion is not affected by the horizontal motion, appears clearly since the duration of the pressure rise-up, as it is not instantaneous, is similar whatever the considered side and whatever the horizontal velocity.

The distribution over the wetted surface is computed according to MLM. The influence of the horizontal velocity is illustrated in the figures (Fig. 10) to (Fig. 12) for $V = 5m/s$, $V = 10m/s$ and $V = 20m/s$. We distinguish positive and negative pressure in the plane (m, Y) with different colors. In addition we multiply the pressure with $\sqrt{1-Y^2}$ so that the change of sign of the pressure appears clearly. For a given size of the elliptic paraboloid, that is to say before separation of the flow occurs, the smaller the horizontal velocity, the latter the negative pressure appears. The superimposed line corresponds to the theoretical limit given by zeroes of the first order pressure (34). The discrepancies between first order pressure and MLM pressure seems to be greater at low horizontal velocity.

E. Force

At the leading order, the vertical force F_z follows from the integration of the pressure along $\vec{z}$. We can check that performing the integration of the pressure over the contact region D yields the same result that

$$F_z = -\rho \frac{\mathrm{d}^2}{\mathrm{d}t^2} \int\int_{D(t)} \phi \mathrm{d}x\mathrm{d}y \tag{61}$$

since both ϕ and its normal derivative on the contour $\partial D(t)$ vanish. By using the expression of the displacement potentiel in (21) and the identities (26), the vertical force (whatever the entering kinematics) is

$$F_z = \frac{4\pi\rho}{15E} \frac{\mathrm{d}^2}{\mathrm{d}t^2} \left[a^2 bh\right] = \frac{4\pi\rho}{15E} k^2 \eta^3 \frac{\mathrm{d}^2}{\mathrm{d}t^2} \left[h^{5/2}\right] \tag{62}$$

It is worth noting that the force depends on time variation of the penetration depth h only since the factor $\frac{k^2\eta^3}{E}$ is a constant and depends on the geometry only. It is rather surprising that the force does not depend on the pressure distribution while the latter strongly depends on the horizontal velocities and varies significantly during the penetration.

Assuming that the vertical velocity W is constant, the force reduces to

$$F_z = \frac{1}{E} \pi\rho k^2 \eta^3 W^{5/2} \sqrt{t} \tag{63}$$

Figure (Fig. 13) compares experimental time variation of the force data (see [10]) and the formula (63) scaled by $W^{5/2}$ As usual the first order formulation (63) overestimates the force.

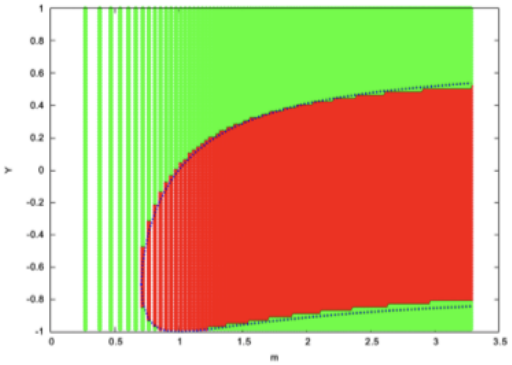

Fig. 12. See caption in (Fig. 10). Horizontal velocity $V = 20m/s$.

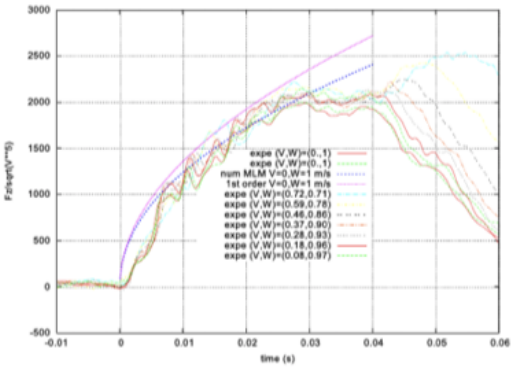

Fig. 13. Time variation of the force scaled with $W^{5/2}$. Comparison with experimental data decsribed in [10].

When the kinematics is a pure vertical motion the computation of the force from a numerical integration of the pressure MLM is detailed in [9]. The corresponding force is plotted in (Fig. 13) as well and a better agreement with experimental data is obtained.

It is worth reminding that the numerical integration is better handled if the position of the vanishing pressure is precisely known in the close vicinity of the contact line. In the present case, it is shown that the area where the pressure is negative starts growing after a while as the body penetrates the fluid. No attemps are made to compare the first order force (62) to the numerical integration of the pressure MLM when the translational velocity exists. However in the experiments mentionned above, the penetration before separation of the flow is far smaller that the time at which $b = V$. In that case MLM results with or without horizontal velocity are very similar.

It is also worth noting that the experimental vertical force starts increasing with a finite slope at initial instant of contact. It is suggested to average the force over a short time duration thus accounting for the fact that force sensor cannot measure instantaneously.

Considering now a free drop of the body. Its mass in air is μ. In the absence of any other hydrodynamic force that the force (62), Newton's law yields a differential equation which can be integrated. The following equation must be solved

$$\mu h + C(e)h^{5/2} = \mu W_o t \tag{64}$$

where W_o is the initial velocity and the factor $C(e)$

$$C(e) = \frac{4\pi\rho(1-e^2)\eta^3(e)}{15E(e)} \tag{65}$$

is a constant only function of the geometry in terms of the aspect ratio k_γ according to (16). In order to illustrate the kinematics during free drop, it is easier to plot the time t in terms of the penetration depth $h(t)$ for given data (μ, e, W_o). The following figure shows such variation

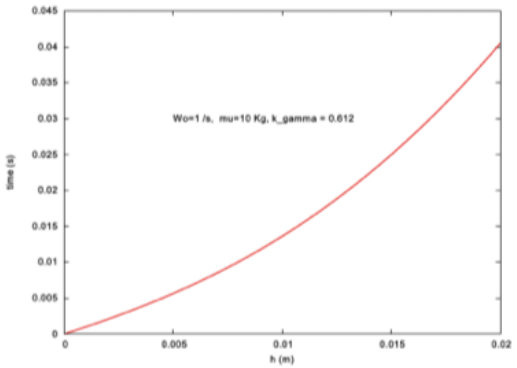

The added mass of the penetrating body reads

$$\mu_a = \frac{5}{2}C(e)h^{3/2} \tag{66}$$

and the acceleration reads

$$\ddot{h} = -\frac{15}{4}C(e)\mu W_o \frac{\sqrt{h}}{(\mu+\mu_a)^2} \tag{67}$$

From equation (30), it is possible to define other circumstances when the pressure calculated at the initial contact point $X = Y = 0$, may vanish during free drops. That occurs when $\dot{M} = 0$, yielding

$$U^2 + k^2V^2 = a^2\overline{\dot{a}\dot{W}} \tag{68}$$

By using Newton's law $(\mu\dot{W} = -\overline{\dot{W}\mu_a})$, and the identity $\dot{\mu_a} = \frac{3\mu_a W}{2h}$ after some algebra, it is shown that if the horizontal kinematics is fitted to the vertical kinematics as follows

$$U^2 + k^2V^2 = \frac{W^2a^3}{2h}\frac{\mu - 2\mu_a}{\mu+\mu_a} \tag{69}$$

the pressure at the initial contact point vanishes thus leading to possible cavitation. If the horizontal velocity is zero, the vanishing pressure occurs when the added mass is twice the mass in air of the body. That result is shown in [11]. Further investigation of a growing cavitation pocket is described in [12].

ACKNOWLEDGMENT

The experimental results shown in this paper have been obtained in a campaign carried out in BGO First (La Seyne/Mer, France) as a part of the European project TULCS: Bureau Veritas, Marin, Compagnie Maritime d'Affrétement – Compagnie Générale Maritime, Canal de Experiencias Hidrodinamicas, Ecole Centrale Marseille, Technical University Delft, University of Zagreb, Technical University of Denmark, University of East Anglia, SIREHNA, WIKKI, HYDROCEAN, Brze Vise Bolje. The experimental campaign has been also supported by GIS Hydro – Conseil Général du var.

APPENDIX A
GALIN'S THEOREM

Theorem: *let the functions* (G, F, P, I) *defined as follows:*

$$G(x,y) = \frac{1}{R} = \frac{1}{\sqrt{x^2+y^2}}, \quad F(x,y) = 1 - \frac{x^2}{a^2} - \frac{y^2}{b^2}, \tag{70}$$

$$P(x,y) = \sum_{p=0}^{M} \sum_{q=0}^{M-p} b_{pq} x^p y^q \tag{71}$$

$$I(x,y) = \int_D \frac{P(x_0,y_0)}{\sqrt{F(x_0,y_0)}} G(x-x_0, y-y_0) \mathrm{d}x_0 \mathrm{d}y_0 \tag{72}$$

then, if $(x,y) \in D = \{(x,y),\ \frac{x^2}{a^2} + \frac{y^2}{b^2} \leq 1\}$,

$$I(x,y) = \sum_{p=0}^{M} \sum_{q=0}^{M-p} a_{pq} x^p y^q \tag{73}$$

that means that I *is a polynomial in* (x,y) *of the same degree as* P.

We assume here that Galin's theorem can be inverted: *If* I *is polynomial in* (x,y)*, say with degree* M*, then* P *is polynomial as well with same degree* M. The expressions of coefficients a_{pq} in terms of b_{pq} are detailed in [1].

REFERENCES

[1] Vorovich I.I., Aleksandrov V.M.and Babeshko V.A, Non-classical Mixed Problems of the Theory of Elasticity, Nauka, Moscow, 1974.

[2] Kalker J.J., Three-dimensional elastic bodies in rolling contact. Kluwer Academic Publisher, 1990.

[3] Scolan Y.-M. and A. A. Korobkin, Towards a solution of the three-dimensional Wagner problem. 23^{rd} International Workshop on Water Waves and Floating Bodies, Korea, 2008.

[4] Scolan Y.-M. & Korobkin A.A., Three-dimensional theory of water impact. Part 1. Inverse Wagner problem. J. Fluid Mech, 440, pp 293-326, 2001.

[5] Korobkin A. A. & Scolan Y.-M., Three-dimensional theory of water impact. Part 2. Linearized Wagner problem. J. Fluid Mech. Vol. 549, 2006.

[6] Korobkin A.A. Penetration of elliptic paraboloid into liquid at a variable velocity. J. Applied Mathematics and Mechanics. Vol. 66, pp. 39-48, 2002.

[7] Scolan Y.-M. and A. A. Korobkin, Hydrodynamic impact (Wagner) problem and Galin's theorem. 27^{th} International Workshop on Water Waves and Floating Bodies, Copenhagen, 2012.

[8] Stephan E.P., Boundary integral equations for mixed boundary value problems in R^3, Math. Nachrichten 134, pp 21–53, 1987.

[9] Korobkin A.A. & S. Malenica, Modified logvinovich model for hydrodynamic loads on asymmetric contours entering water, 20^{th} International Workshop on Water Waves and Floating Bodies, Spitzbergen, Norway, 2005.

[10] Scolan Y.-M., European project TULCS (Tools for Ultra Large Container Ships), Second campaign in BGO, 2012.

[11] Scolan Y.-M., Low pressure occurence during free fall of a three-dimensional body onto a liquid free surface, Euromech 450, IRPHE, 2004.

[12] Korobkin A.A., Cavitation in liquid impact problem. Proc. 5th Intern. Congress on Cavitation, Osaka, Japan, 2003.

[13] Wagner, H., Über Stoss- und Gleitvorgänge an der Oberfläche von Flüssigkeiten. *ZAMM* **12**, pp. 193-215, 1932.